Extended Abstracts of the 1999 International Conference on Solid State Devices and Materials, Tokyo, 1999, pp. 8-9 **A-1-1**

Effects of the Scaling on n+/p Junction Leakage Characteristics

T. Fukai, K. Takeuchi and T. Mogami
ULSI Research Lab., Silicon Systems Research Labs., NEC
1120 Shimokuzawa, Sagamihara, Kanagawa 229-1198, JAPAN
Phone: +81-42-779-9930, Fax: +81-42-771-0886

1. Introduction

As the dimensions of DRAM cells continue to be reduced, the p-n junction leakage will become a more serious problem due to the increase of the substrate doping and refreshing interval. Therefore, to further enlarge the DRAM capacity, quantitative understanding of the junction leakage is essential. In this work, the leakage current characteristics are measured for a wide range of substrate concentrations and compared with theoretical models. Then, the leakage behavior towards sub-0.1μm DRAM cells is discussed.

2. Experimental Results

N+/p junctions were fabricated, varying the substrate concentration N_{SUB} between 2E17cm^{-3} and 1.8E18cm^{-3}. Boron was implanted and deeply diffused at 1200°C into the substrate to form flat p-type doping profiles. The n-type diffusion layers were formed either by ion implantation (As or P, 4E13cm^{-2} or 3E15cm^{-2}) or solid phase diffusion from PSG. N+ activation / diffusion was performed by RTA. To minimize the damage, contact holes were opened by wet etching and filled with *in situ* phosphorous-doped poly-silicon.

Fig.1 shows the leakage current distributions within a wafer for various substrate concentrations. The leakage current increases as N_{SUB} increases. It is also noted that minority tail distributions appear at the higher doping cases. Fig.2 shows the I-V characteristics of the samples shown in Fig.1. While the voltage dependence is relatively weak below 5E17cm^{-3}, sudden increase of the leakage in the high bias range occurs around 1E18cm^{-3}. This increase is accompanied by the appearance of the tail distributions in Fig.1. The dashed line is an I-V curve of a sample belonging to the tail. The current deviation occurs only in the intermediate voltage range.

3. Explanation by Theory

To quantitatively understand the above results, corresponding I-V characteristics were calculated using physically based models. The basic leakage mechanisms considered are diffusion, field-enhanced generation (FEG), and Zener (band-to-band) tunneling. FEG is the SRH generation process enhanced by the electric field, where an effective emission barrier lowering, due to the tunneling through the triangular potential, is considered[1]. FEG and Zener current were calculated using the equations in Table.1. Eq.2 is based on the work in [2].

Fig.3 compares the measured and calculated I-V characteristics. Very good agreement was obtained. In the low electric field conditions, FEG dominates, exhibiting the weaker voltage dependence. Zener current with stronger voltage dependence appears in the high field conditions. For the calculation, field distributions F(z) were determined by process and device simulation. The important fitting parameters are m* for FEG (=0.30m_0), m* for Zener (=0.33m_0), and the density of traps for area (N_{TA}[cm^{-3}]) and perimeter (N_{TP}[cm^{-2}]) FEG. By only adjusting N_{TA} and N_{TP}, the I-V characteristics for a wide range of substrate doping and area vs. perimeter ratio can be reproduced.

To account for the leakage fluctuation, a local Zener (LZ) model[3] was further included. The model assumes that small precipitates (metal or dielectric) locally distort the electric flux and enhance the electric field. The I-V characteristics of the deviated junctions can be explained by assuming the existence of precipitates, as shown in Fig.4. The deviation occurs only when F is sufficiently large, in agreement with Fig.1, because substantial current increase can occur only when the locally increased F is high enough to induce Zener current.

Fig.5 shows the measured and calculated temperature dependence of the leakage current. Good agreement is again confirmed for all the N_{SUB} range and both normal and degraded junctions.

4. Discussion

Fig.6 shows the effective density of generation-related traps N_{TA} and N_{TP} extracted by fitting the FEG-dominated I-V curves to the model. N_{TA} increases with the substrate concentration. A possible reason would be the shift of the junction depth towards the surface, where higher trap density is expected. N_{TP} shows weaker N_{SUB} dependence, suggesting different origin of the traps (possibly surface states). From these results, the cause of the leakage increase with N_{SUB} can be estimated as shown in Fig.7. In this particular case, both the increase of field and trap density does comparable contribution to the leakage increase.

Using the models, the junction leakage in scaled DRAM cells was projected (Fig.8), assuming the feature size is proportional to $N_{SUB}^{-1/2}$. The FEG current is almost constant, because of the balance between the increase of F and decrease of the perimeter. The intrinsic Zener current is not significant for N_{SUB} up to 5E18cm^{-3}. However, if precipitates exist (1nm^3 effective volume), sharp increase of the leakage occurs even at 1E18cm^{-3}. Therefore, the elimination of the precipitates is very important for further DRAM scaling. It was found that the PSG junctions significantly reduce the leakage fluctuation, as shown in Fig.9, suggesting that the precipitates were introduced by ion implantation. Measures to reduce the implanted contamination, such as the solid phase diffusion, will be necessary for the future DRAM production.

5. Conclusion

The combination of FEG, Zener and Local Zener models clearly explain the measured n+/p junction leakage characteristics for a wide range of substrate concentration, bias and temperature. Using the models, it is predicted that the control of precipitates is especially important to realize sub-0.1μm DRAM cells.

References

[1] G.Vincent et al., J. Appl. Phys. 50, p.5484, 1979.
[2] E. O. Kane, J. Appl. Phys., 32, p.83, 1961.
[3] K. Ohyu et al., IEEE Trans. Electron Devices, 42, p.1404, 1995.

Table 1. FEG and Zener current expressions.

FEG

$$G' = G\left[1+\int_{0}^{E_t/kT} exp\left\{z - z^{3/2}\left(\frac{4}{3}\frac{\sqrt{2m^*}(kT)^{3/2}}{q\hbar F}\right)\right\}dz\right] \quad \text{(Eq.1)}$$

Zener tunneling

$$J = q\cdot F\frac{1}{(2\pi)^3}\frac{4\pi q m_{hd}}{\hbar^3}\cdot exp\left[-\frac{\pi m^{*1/2}E_g^{3/2}}{2\sqrt{2}q\hbar F}\right]\cdot\frac{1}{2}\cdot\frac{4\sqrt{2}q\hbar F}{3\pi m^{*1/2}E_g^{1/2}} \quad \text{(Eq.2)}$$

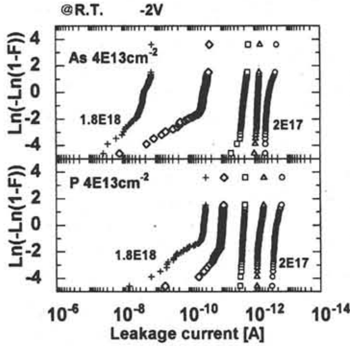

Fig.1 Distributions of n+/p junction leakage current within wafers at -2V. Junction size is 500μm×200μm. N_{SUB}=1.8E18, 1.4E18, 8E17, 5E17 and 2E17 cm^{-3}.

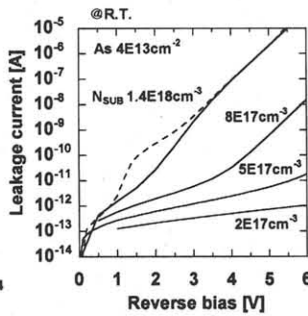

Fig.2 I-V characteristics of the samples in Fig.1. Dashed line is for a sample belonging to the tail distribution.

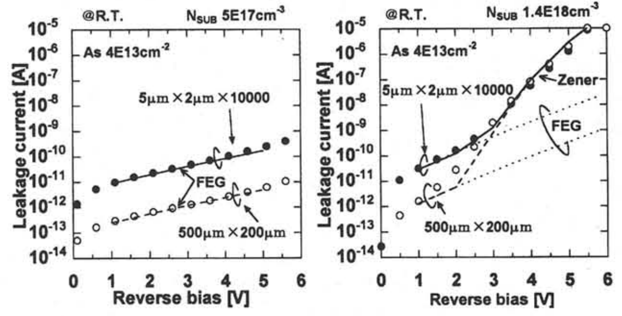

Fig.3 Comparison of measured (dots) and calculated (lines) I-V characteristics. Note that, while FEG current depends on the perimeter, Zener current does not.

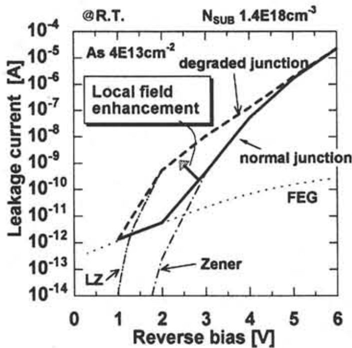

Fig.4 Calculated junction I-V characteristics with and without precipitates.

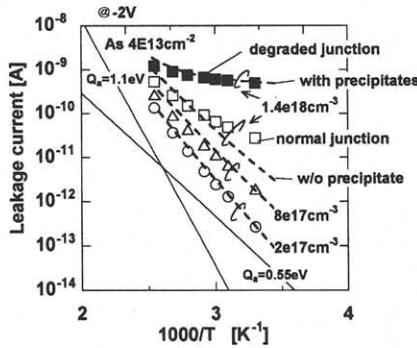

Fig.5 Comparison of the measured (dots) and calculated (lines) temperature dependence of junction leakage.

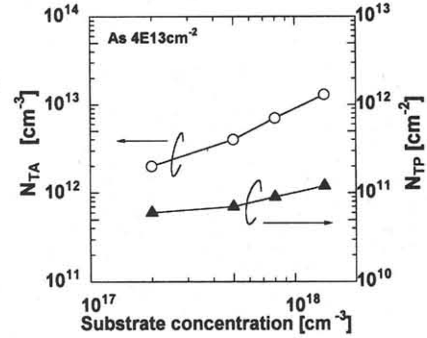

Fig.6 Extracted area (N_{TA}) and perimeter (N_{TP}) trap densities vs substrate concentration.

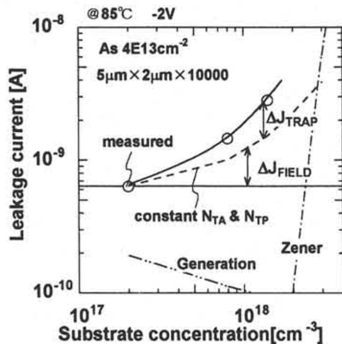

Fig.7 Estimated contributions of field (ΔJ_{FIELD}) and trap density (ΔJ_{TRAP}) to measured leakage increase. Sample size is fixed (5μm×2μm×10000).

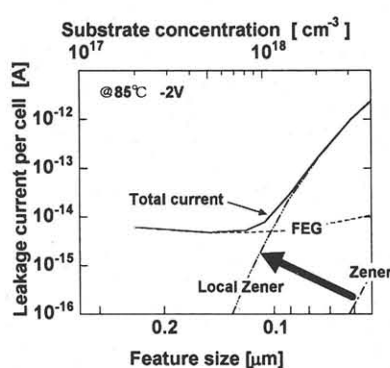

Fig.8 Projected junction leakage vs DRAM cell feature size. Local Zener current will become serious even at N_{SUB} of 1E18cm^{-3}

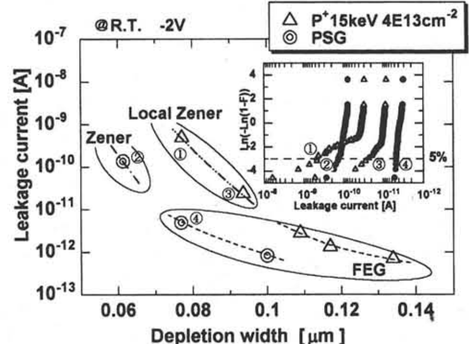

Fig.9 Leakage current at cumulative probability of 5% vs measured depletion region width, for PSG and P+ implanted samples.